Why are organic micropollutants not fully biotransformed? A mechanistic modelling approach to anaerobic systems

Lorena Gonzalez-Gil, Miguel Mauricio-Iglesias*, Marta Carballa, Juan M. Lema

Department of Chemical Engineering, School of Engineering, Universidade de Santiago de Compostela, Rúa Lope Gómez de Marzoa, E-15782 Santiago de Compostela, Spain

* Corresponding author

E-mail addresses: lorena.gonzalez@usc.es, miguel.mauricio@usc.es, juan.lema@usc.es, marta.carballa@usc.es

Graphical abstract

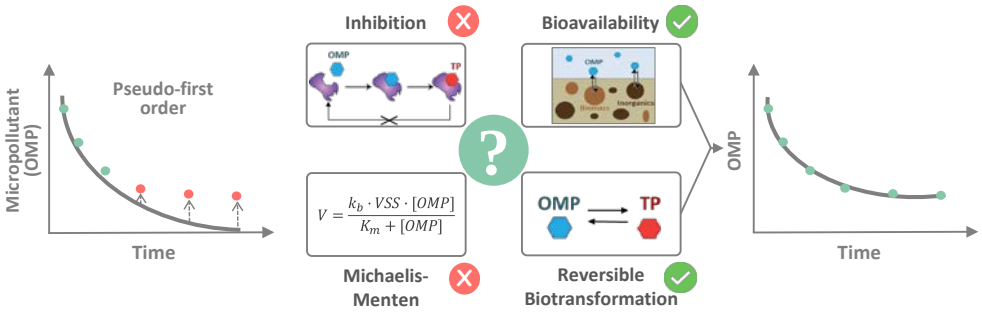

Abstract

Biotransformation of most organic micropollutants (OMPs) during wastewater treatment is not complete and an unexplained steady decrease of the biotransformation rate with time is reported for many OMPs in different biological processes. To minimize and accurately predict the emission of OMPs into the environment, the mechanisms and limitations behind their biotransformations should be clarified. Aiming to achieve this objective, the present study follows a mechanistic modelling approach, based on the formulation of four models according to different biotransformation hypotheses: Michaelis-Menten kinetics, chemical equilibrium between the parent compound and the transformation product (TP), enzymatic inhibition by the TP, and a limited compound bioavailability due to its sequestration in the solid phase. These models were calibrated and validated with kinetic experiments performed in two different anaerobic systems: continuous reactors enriched with methanogenic biomass and batch assays with anaerobic sludge. Model selection was conducted according to model suitability criteria (goodness of fitting the experimental data, confidence of the estimated parameters, and model parsimony) but also considering mechanistic evidences. The findings suggest that reversibility of the biological reactions and/or sequestration of compounds are likely the causes preventing the complete biotransformation of OMPs, and biotransformation is probably limited by thermodynamics rather than by kinetics. Taking into account its simplicity and broader applicability spectrum, the reversible biotransformation is the proposed model to explain the incomplete biotransformation of OMPs.

Keywords: bioavailability, biotransformation mechanism, incomplete removal, mathematical modelling, parameter estimation, pharmaceuticals

1. INTRODUCTION

A wide variety of organic compounds, such as pharmaceuticals, personal care products, polycyclic aromatic hydrocarbons (PAH), industrial chemicals and pesticides, are released worldwide into the environment through agriculture, industry and domestic practices. These emerging pollutants are collectively known as organic micropollutants (OMPs) and have been detected in sewage, surface, ground, drinking water (Luo et al., 2014) and in biosolid-amended soils (Chen et al., 2014). Although OMPs are present at trace concentrations, some compounds represent a potential risk to human health and the environment due to their persistence and bioaccumulation (Tiwari et al., 2017; Tousova et al., 2017).

Biological treatment processes are considered the most cost-effective alternative to remove OMPs by biotransformation (Grandclément et al., 2017) and even to reduce the toxicity of wastewaters (Völker et al., 2017). However, in most wastewater treatment plants (WWTPs) unsatisfactory removal is attained (Falås et al., 2016). In order to minimize the emission of OMPs into the environment, it would be helpful to clarify the mechanisms and limitations behind their biotransformations. Suárez et al. (2008) and Tiwari et al. (2017) suggest that the main factors influencing the biotransformation are operational parameters (retention time, temperature and pH), microbial community, bioavailability and physicochemical properties of OMPs. Several attempts pursuing 100% biotransformation efficiency have been performed modifying operational conditions and the microbial community of the biological treatment processes; nevertheless, in most cases, these strategies were unsuccessful or led to contradictory results (Luo et al., 2014; Stasinakis, 2012; Suárez et al., 2008; Tiwari et al., 2017).

Incomplete biotransformation has been observed for a wide variety of OMPs in several biological systems and actually biotransformation almost stops at one point leading to steady remaining concentrations of OMPs identified as kinetic plateaus. These plateaus were reported for OMPs with aliphatic amines in activated sludge batch experiments (Gulde et al., 2018) and for other OMPs with diverse physicochemical characteristics (Blair et al., 2015). Likewise, Fernandez-Fontaina et al. (2014) found a similar kinetic trend for fluoxetine biotransformation in continuous nitrifying reactors and Xue et al. (2010) observed quasi-plateaus for several OMPs with aerobic biomass from an anaerobic/anoxic/aerobic-membrane bioreactor. In a previous study (Gonzalez-Gil et al., 2018), we reported how the estimated biotransformation of various OMPs virtually stopped in anaerobic continuous experiments with enriched methanogenic biomass. These results suggest that the appearance of concentration plateaus is somehow independent of the biological system (aerobic/anaerobic), the phase partitioning of the OMP (liquid and/or solid), or even the biotransformation mechanism (cometabolism/metabolism). Moreover, this behavior cannot be explained by the typically assumed pseudo-first order kinetic.

Mathematical models can describe the biotransformation kinetics of OMPs and be used with a three-fold objective: to obtain a further insight on the mechanisms leading to their biotransformation, to incorporate OMP removal criteria in process design, and to effectively predict the release of OMPs on the receiving environment. Although a wide variety of models have been reported to depict the fate of OMPs in activated sludge processes (Pomiès et al., 2013), few have been applied to anaerobic systems and they were focused exclusively on PAH (Barret et al., 2010a, 2010b; Delgadillo-Mirquez et al., 2011). These authors observed a strong correlation between PAH and dry matter removal rates during AD, thus their models are based on the cometabolic kinetics proposed by

Criddle (1993). However, dependency between substrate uptake rate and OMP biotransformation has not been found for other kind of OMPs during AD, e.g. pharmaceuticals and personal care products (Gonzalez-Gil et al., 2018), hence being necessary to formulate new models. To the best of our knowledge, no study has addressed the kinetic and/or thermodynamic limitations that lead to a halt in OMP biotransformation (i.e., appearance of concentration plateaus).

This study intends to gain further insights about biotransformation mechanisms and limitations that could contribute to answer the question: why are OMPs not fully biotransformed? To achieve this, sound mechanistic models describing experimental data of anaerobic biotransformation of 20 OMPs have been proposed and evaluated, trying to identify the most suitable one. Although this study focuses on anaerobic systems, the employed methodology and the resulting conclusions aim to be applicable to other biological wastewater treatments. Finally, the implications of using an accurate model to describe OMP removal in anaerobic process design are discussed.

2. MATERIALS AND METHODS

2.1 Organic micropollutants

A set of 20 OMPs (Table 1) usually detected in sewage sludge (Gonzalez-Gil et al., 2016; Paterakis et al., 2012; Stasinakis, 2012), with different sorption and biotransformation characteristics in anaerobic systems (Gonzalez-Gil et al., 2018) and representative of a wide range of OMPs were selected in this study. Stock solutions were prepared in HPLC grade methanol or acetone, depending on the compound, and stored at -18 °C.

Table 1. Groups of OMPs studied according to their sorption (partition coefficient, K_d) and biotransformation characteristics under methanogenic conditions.

Group 1 *Lipophilic (log K_d > 2.5)* *Biotransformation: 40-70%*	**Group 2** *Medium hydrophobicity (2.5 ≥ log K_d ≥ 2)* *Biotransformation: 30-60%*
Galaxolide (GLX)	Bisphenol A (BPA)
Tonalide (TON)	Estrone (E1)
Celestolide (CEL)	17β-estradiol (E2)
Fluoxetine (FLX)	17α-ethinylestradiol (EE2)
Triclosan (TCS)	Diazepam (DZP)
4-octylphenol (OP)	
4-nonylphenol (NP)	
Group 3 *Hydrophilic (2 > log K_d > 1)* *Biotransformation <60%*	**Group 4** *Hydrophilic (2 > log K_d > 1)* *Biotransformation >70%*
Ibuprofen (IBP)	Sulfamethoxazole (SMX)
Naproxen (NPX)	Trimethoprim (TMP)
Diclofenac (DCF)	
Erythromycin (ERY)	
Roxithromycin (ROX)	
Carbamazepine (CBZ)	

2.2 Kinetic experiments in continuous methanogenic reactors

The data used for evaluating the models were obtained in three independent kinetic experiments performed in two mesophilic (37 ºC) continuously stirred lab-scale reactors (15 L) inoculated with biomass from a mesophilic sewage sludge digester and fed with a mixture of volatile fatty acids (hydraulic retention time, HRT=10 d; organic loading rate, OLR=1-2 g COD/L d) to achieve a specific acetogenic-methanogenic biomass with no hydrolytic-acidogenic activity. The operational conditions are described in detail elsewhere (Gonzalez-Gil et al., 2018) and briefly explained here for the sake of completeness. Each kinetic experiment was initiated by adding a pulse of the selected OMPs to the corresponding methanogenic reactor (MR, operating in steady-state) to attain an initial in-reactor concentration of approximately 10 µg/L for hormones (E1, E2, and EE2) and 100 µg/L for the rest of compounds. The OMP concentrations in the liquid

(8 time points) and solid phases (5-6 time points) were monitored for 7-9 d (Gonzalez-Gil et al., 2018). During this time the reactor operation (and feeding) was kept in a continuous mode. The model parameters (calibration) were estimated using the results from two kinetic experiments (Experiment 1 and 2) performed in the same reactor (suspended solids, TSS=9.3 g/L; volatile suspended solids, VSS=3.0 g/L). A new set of data (Experiment 3), obtained in an independent methanogenic reactor (TSS=8.9 g/L, VSS=2.2 g/L), was employed for model validation. The differences among the three kinetic experiments are further discussed by Gonzalez-Gil et al. (2018).

2.3 Kinetic experiments in batch anaerobic digesters

In order to additionally test the mechanistic applicability of the mathematical models previously evaluated with the kinetic methanogenic experiments (Experiments 1-3), kinetic batch assays were carried out with biomass from a mesophilic lab-scale anaerobic digester (HRT of 20 d and OLR around 2.0 g COD/L d) treating sewage sludge, and thus containing microorganisms involved in the four AD steps (hydrolysis, acidogenesis, acetogenesis and methanogenesis). Sixteen independent bottles of 350 mL were inoculated (37 °C and 135 rpm) with anaerobic biomass (TSS=13 g/L, VSS=7.9 g/L) and spiked with the OMP (100 μg/L, except for hormones 10 μg/L) to measure 8 time points in duplicate (one bottle per sample) for 14 d (Experiment 4). Apart from the remaining substrate of the digestate, no additional feeding was added to these bottles; thus, a low methane production (100 mL) and COD removal (around 6%, Figure S1) was achieved after 14 d. The pH was approximately 7.5 along the whole experiment and no accumulation of VFA was observed. This experimental procedure ensured a constant anaerobic activity and VSS concentration during the whole batch experiment; therefore, the appearance of concentration plateaus could not be explained by a decrease in the biomass activity.

The total concentration (solid+liquid) of the OMPs in Experiment 4 was followed applying ultrasonic solvent extraction (USE) to the freeze-dried sludge (approximately 0.5 g). After five series of solvent extractions with ultrasounds, the supernatants were combined, concentrated and then, diluted with distilled water, before performing solid phase extraction (SPE) with 200 mg OASIS HLB cartridges (Waters, Milford, MA, USA). One half of the OMPs studied (IBP, NPX, DCF, BPA, TCS, NP, OP, HHCB, AHTN, ADBI) were determined using Gas Chromatography coupled to Mass Spectrometry (GC-MS), whereas the rest of micropollutants (FLX, CBZ, DZP, ERY, ROX, SMX, TMP, E1, E2, EE2) were quantified using Liquid Chromatography coupled to Mass Spectrometry (LC-MS/MS). Further details for the OMPs quantification are given by Gonzalez-Gil et al. (2016).

Total and partial alkalinity, pH, total and soluble COD, TS, VS, TSS and VSS were monitored according to standard methods (APHA, 2005). The concentration of volatile fatty acids (acetic, propionic, butyric) was determined using a gas chromatograph (HP 5890A) with a Flame Ionization Detector (HP 7637A). Biogas production was measured daily with a pressure transducer (Centrepoints electronics) and its composition was determined through gas chromatography (HP 5890 Series II).

2.4 Methodology for model formulation and selection

Given the complex task of evaluating many alternatives with experimental data of the biotransformation of 20 OMPs, a stepwise method (Figure 1) was proposed to formulate, test and ultimately select a mechanistic model describing the experimental results. The rationale followed aimed to assist decision making in formulating model alternatives and selecting the most plausible candidate. All the individual tasks are briefly explained below.

First, based on physicochemical and biological principles (specified in section 3.3), different models are formulated, generally as sets of mass balances represented by a system of ordinary differential equations (ODEs). Secondly, the model alternatives are evaluated by fitting to the biotransformation kinetics of four representative OMPs (Experiments 1-2) with different biotransformation and sorption behavior (Table 1). The motivation for using only four OMPs is to include visual inspection as an important criterion in model selection besides quantitative indexes. If no model alternative fits the data satisfactorily, new mechanistic models can be proposed. After this first screening, the number of model candidates is limited to a few and it is possible to estimate the model parameters (model calibration) for all the OMPs (Experiments 1-2).

Once parameters of all OMPs were determined, they were used to validate the candidate model through simulation of an independent set of experimental data (Experiment 3). Likewise, the applicability of the mechanistic model candidates to other biological systems can be verified by using these models to fit new kinetic data obtained in other biological processes (Experiment 4). The information obtained in the three previous steps (calibration, validation and verification) allows to decide whether any model candidate is appropriate to explain and predict the OMP behavior or if, on the contrary, it is necessary to formulate additional mechanistic models.

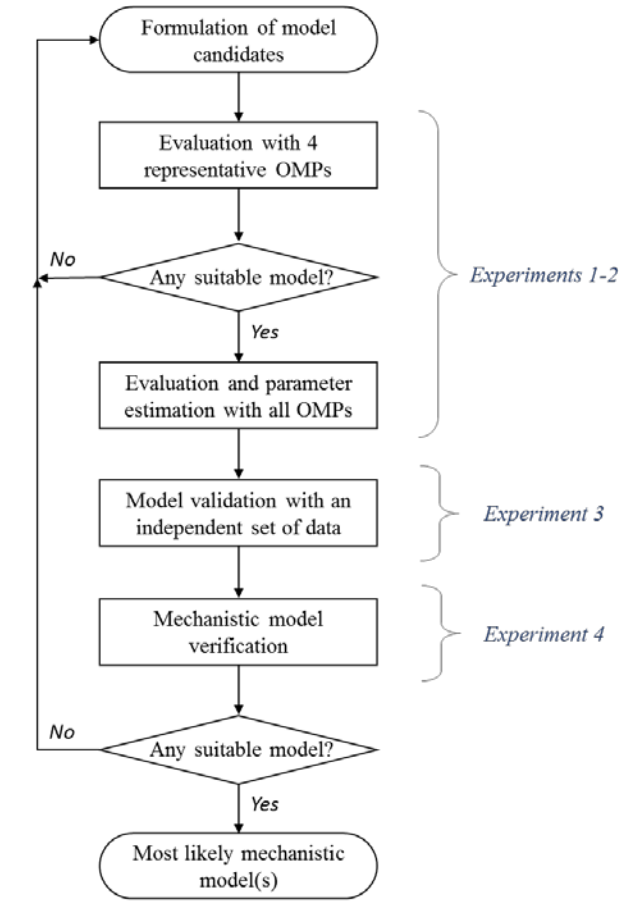

Experiment	Continuous	Batch	Methanog.	AD
1-2	X		X	
3	X		X	
4		X		X

Figure 1. Steps followed for the proposal and evaluation of mechanistic models. AD stands for the overall anaerobic digestion process.

2.5 Parameter estimation and model selection criteria

Models were implemented in Matlab® 7.12.0 (R2011a) (Mathworks Inc., Natick, MA, USA). All the computer files are available upon request to the corresponding author.

2.5.1 Model calibration

Parameter estimation for each model was carried out by minimization of the normalized root squared mean error (Eq. (1)) between the experimental data and the data predicted by the model.

$$NRMSE = \frac{\sqrt{\frac{1}{m \cdot n}\sum_{k=1}^{m}\sum_{i=1}^{n}\left(C_{exp,k}(t_i) - C_{pred,k}(t_i,\theta)\right)^2}}{C_{in}} \cdot 100 \quad (1)$$

where m is the number of variables measured (in this case, m=2: OMP concentration in solid and liquid phase), n is the number of sample times, $C_{exp,k}$ is the measured value, $C_{pred,k}$ is the value predicted by the model, θ represents the vector of calibration parameters for a given model, and C_{in} is the initial concentration of OMPs (100 μg/L, except for hormones 10 μg/L). It was considered that the errors of measured concentrations in liquid and solid phase were similar and no weighting was needed.

To ensure the robustness of the calibrated parameters and prevent being stuck at local minima caused by poor initial guesses, we performed a bootstrap method to determine the expected value and the confidence interval of the parameter (Frutiger et al., 2016). The bootstrap steps are detailed in Supporting Information section S2 and succinctly described here. Firstly, a reference parameter estimation was carried out in order to estimate reference residuals. These residuals were used to generate simulated experimental data and repeat the parameter estimation, now based on these simulated concentrations. Iterating through the previous steps until convergence, a population of parameters is obtained that can be used to reach robust estimates and quantifications of uncertainty.

2.5.2 Validation and prediction uncertainty

Based on the parameters estimated through the bootstrap method, a third independent set of experimental data ($C_{val,k}$) was used for model validation, which was quantified based on the validation NRMSE (Eq. (1), where $C_{exp,k}$ is replaced by $C_{val,k}$).

The uncertainty of the model predictions was plotted for visual inspection of the match between simulated and experimental data. A Monte Carlo procedure was followed based on propagating the uncertainty of the previously estimated parameters. Latin Hypercube Sampling (Helton and Davis, 2003) was used to provide samples of the parameter space maximizing its coverage. The Monte Carlo procedure consisted of i) drawing a random sample of the estimated parameter space; ii) simulating the model and storing the predictions; iii) iterating 200 times steps i) and ii) until the distribution of model outputs converges.

2.5.3 Model comparison and selection

The models proposed for testing have different number of parameters and, in general, are non-nested, i.e. a reduced model is not equivalent to setting a constant parameter in more complex model. For non-nested parameters, it is recommended to use Akaike's Information Criterion (AIC) for model comparison and selection instead of the NRMSE, which provides complementary information about the goodness of the model prediction. Assuming that errors are close to be identically and normally distributed, AIC can be determined by Eq. (2).

$$AIC = m \cdot n \, log\left(\frac{RSS}{m \cdot n}\right) + 2\,p \tag{2}$$

where p is the number of free parameters of each model and *RSS* is the residual sum of squares that can be calculated as $RSS = RMSE^2\, m \cdot n$. The model with lowest AIC can be considered as the most likely candidate to reproduce the experimental results while avoiding overparameterisation.

3. FORMULATION OF MECHANISTIC MODELS

3.1 Two compartment model

Removal of OMPs in anaerobic systems depends mainly on biotransformation and sorption onto sludge. Volatilization to biogas is disregarded, since this mechanism has been reported to have a negligible impact, even in the case of musk fragrances (Alvarino et al., 2014). Therefore, all the proposed models were at least composed of two compartments (liquid and solid phase) linked by sorption (Eq. (3)) and desorption (Eq. (4)) occurring simultaneously. When the rates of these two transport processes with opposite directions equalize, the sorption equilibrium is reached and the solid-liquid partition coefficient (K_d, Eq. (5)) is an appropriate parameter to describe sorption of OMPs at low concentrations.

$$j_{sor} = k_{sor} \cdot X_{TSS} \cdot C_w \quad (3)$$

$$j_{des} = k_{des} \cdot C_s = k_{sor} / K_d \cdot C_s \quad (4)$$

$$K_d = \frac{k_{sor}}{k_{des}} = \frac{C_s}{C_w \cdot X_{TSS}} \quad (5)$$

where j_{sor} is the micropollutant sorption rate (µg/L d), k_{sor} is the sorption kinetic constant (L/gTSS d), j_{des} is the desorption rate (µg/L d), k_{des} is the desorption kinetic constant (1/d), X_{TSS} is the total suspended solids concentration (g/L), K_d is the solid-liquid partition coefficient (L/g TSS), C_w is the concentration of OMP in the liquid phase (µg/L), C_s is the concentration of OMP in the solid phase (µg/L).

Assuming that i) the reactor is well-mixed for both liquid and solid phases; ii) the reactor hold-up and feed flow rate are constant; iii) the OMPs are only added to the reactor as an instantaneous spike (no continuous feed of OMP); and iv) there is a continuous OMP washout from the reactor, since it is operating in a continuous mode, the dynamic mass balances of the OMPs can be written generically as Eq. (6) and (7).

$$\frac{dC_w}{dt} = -\frac{C_w}{HRT} - j_{sor} + j_{des} - r_w \quad (6)$$

$$\frac{dC_s}{dt} = \frac{C_s}{HRT} + j_{sor} - j_{des} - r_S \quad (7)$$

where *HRT* is hydraulic retention time (d), r_w is the biotransformation rate in the liquid phase (µg/L d), and r_s is the biotransformation rate in the solid phase (µg/L d).

3.2 Biotransformation compartment

The compartment where OMP biotransformation occurs is a controversial topic in literature. Most biokinetic models consider that the biotransformation takes place only in liquid phase (Pomiès et al., 2013), and assume that a sorbed compound is not available for microbial degradation (Delgadillo-Mirquez et al., 2011). On the contrary, several evidences support that biotransformation of the sorbed OMPs is possible. For instance, the biotransformation of lipophilic compounds would be limited by partitioning between the two phases if it only occurred in the liquid phase (Fountoulakis et al., 2006). Several extracellular (i.e. hydrolases) and intracellular enzymes (i.e. hydrolases, acetate kinase and monooxygenases) are able to biotransform OMPs in different biological systems (Fernandez-Fontaina et al., 2016; Fischer and Majewsky, 2014; Gonzalez-Gil et al., 2017; Krah et al., 2016); since the small size of most OMPs (<500 Da) allow them to diffuse through the outer membrane of bacteria (Nikaido and Vaara, 1985) they can also be biotransformed inside cells. Lolas et al. (2012) have already demonstrated by radioactive experiments that *Methylobacillus* is able to metabolize TCS accumulated inside the cells. Banihashemi and Droste (2014) suggest that, as biodegradation can also occur when OMPs are sorbed onto the biomass, this transformation mechanism should be incorporated to the existing fate models.

Some studies have already included solid phase biotransformation, with independent or the same rates as in the liquid phase, to achieve a successful calibration of the

mathematical models (Byrns, 2001; Pomiès et al., 2013; Urase and Kikuta, 2005; Xue et al., 2010). To test the various hypotheses in literature, it was considered in this study that biotransformation of OMPs could take place in both the liquid and solid phase of sludge with different ($k_{bw} \neq k_{bs}$) or equal kinetic constants ($k_{bw} = k_{bs}$, parameters defined in Eq. (8) and (9)).

3.3 Biotransformation mechanisms

Although pseudo-first order kinetics cannot reproduce kinetics where the biotransformation rate drastically slows down or comes to a halt (Blair et al., 2015; Fernandez-Fontaina et al., 2014; Gonzalez-Gil et al., 2018), it was considered as a reference (null hypothesis) in this study, since it is widely used to model OMP biotransformation in biological wastewater treatments (Pomiès et al., 2013). The pseudo-first order biotransformation rate depends on the OMP concentration and on the total concentration of VSS as the share of biomass capable of transforming OMPs is not measurable experimentally (Eq. (8) and (9)).

$$r_w = k_{bw} \cdot X_{VSS} \cdot C_w \quad (8)$$

$$r_S = k_{bs} \cdot X_{VSS} \cdot C_s \quad (9)$$

where X_{VSS} is the volatile suspended solids concentration (g/L); k_{bw} is the liquid biotransformation kinetic constant (L/g VSS d) and k_{bs} the solid biotransformation kinetic constant (L/g VSS d).

Four hypotheses were formulated (Figure 2) that can potentially explain the mechanism behind the incomplete removal of OMPs: i) the biotransformation follows a Michaelis-Menten kinetics (Liu et al., 2015), thus the biotransformation rate could substantially slow down at the end of the experiment depending on the Michaelis constant and OMP concentration; ii) the transformation products (TPs) inhibit the enzyme(s) responsible for

biotransformation; iii) as biological reactions are rarely irreversible (Meyers, 1995), the net biotransformation stops when chemical equilibrium is reached between the parent compound and the TP; and, iv) the bioavailability of the compound is restricted because only a fraction of the sorbed OMPs is ready to be biotransformed while the remaining fraction is sequestrated onto the solids, and thus inaccessible to organisms and extracellular enzymes (Brion and Pelletier, 2005). Although sequestration might be considered as an irreversible process, desequestration rate in biological reactors might be significant if OMPs are sequestered in organic matter that is further degraded and/or if OMPs are trapped in microorganisms (Gulde et al., 2018) and hence liberated after cell death. Therefore, the desequestration hypothesis was included in the model formulation. Hypotheses i) and ii) relate to kinetic limitations while the reversible and sequestration models respond to thermodynamic constraints.

Biotransformation may also be limited by enantioselective transformation as recently hypothesized by Polesel et al. (2017); i.e., each enantiomer has a different biotransformation rate to explain the two-rate pattern observed when concentration plateaus appear. Nevertheless, we have not further explored this possibility because the behavior of chiral and non-chiral OMPs was similar (Gonzalez-Gil et al., 2018).

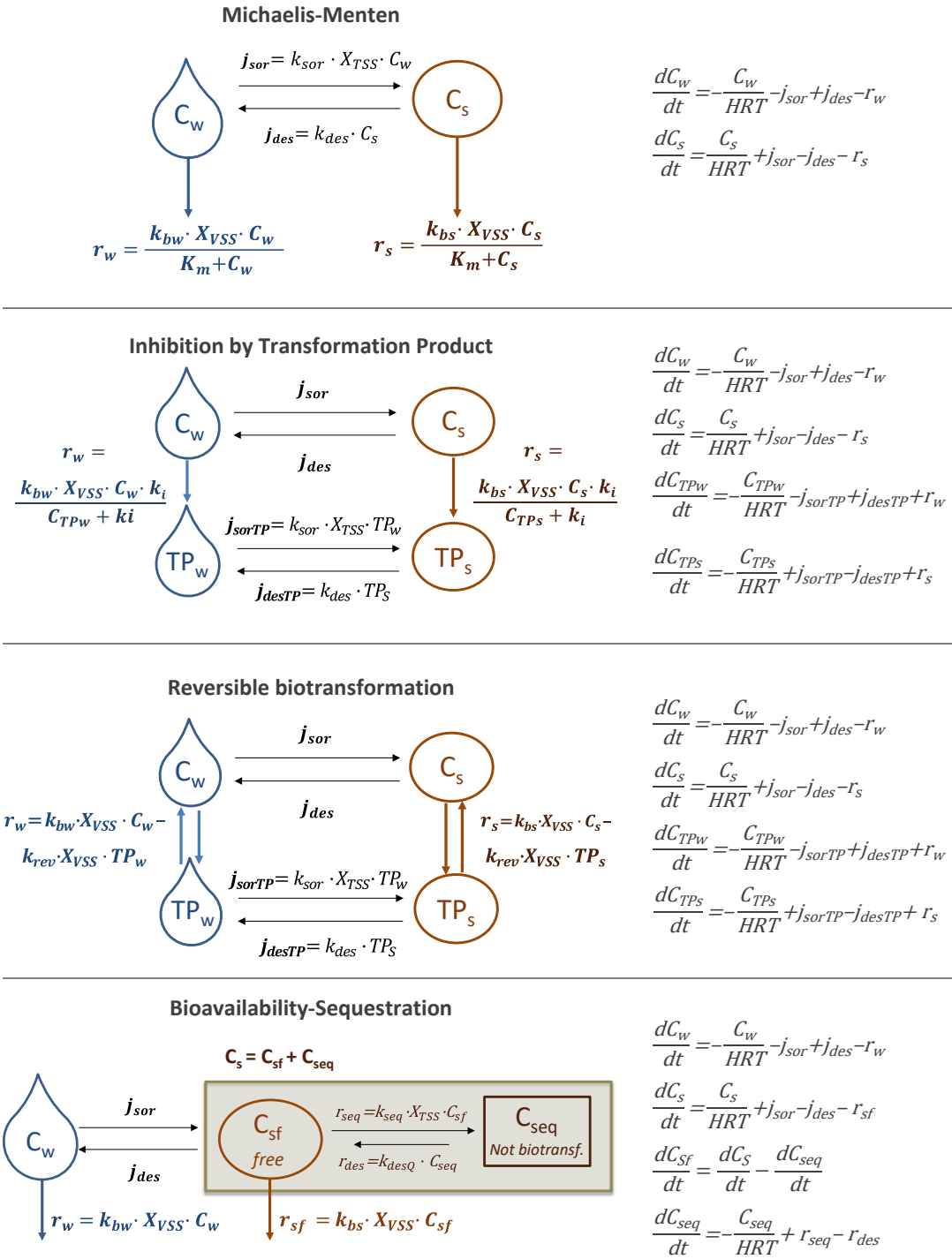

j_{sor}: *Eq. (3)*; j_{des}: *Eq. (4)*; C_{TPw}: concentration of the TP in the liquid (µg/L); C_{TPs}: concentration of the TP in the solid (µg/L); C_{Sf}: solid concentration of bioavailable OMP (µg/L); C_{seq}: concentration of sequestrated OMP (µg/L); K_m: Michaelis-Menten constant (µg/L); k_i: inhibition constant (µg/L); k_{rev}: reversible biotransformation constant (L/g VSS d); k_{seq}: sequestration constant (L/g VSS d); k_{desQ}: desorption constant of sequestered OMP (µg/L).

Figure 2. Schematic representation of formulated models and corresponding mass balances.

4. RESULTS

4.1 Initial model screening

The initial screening intended to verify whether different biotransformation kinetics in the liquid and in the solid compartments were required and if any of the mechanistic models could be ruled out. Three criteria were employed: graphical inspection of biotransformation trends (Figures S3), the NRMSE (Table 2) to quantify the goodness of the experimental data fitting, and the AIC (Table 2) as a criterion for weighting model complexity. FLX (Group 1), E1+E2 (Group 2), ERY (Group 3), and SMX (Group 4) were selected as the four representative OMPs to perform this initial model screening. It should be noticed that E1 and E2 are evaluated jointly because E1 is reduced to E2 under anaerobic conditions.

Each of the mechanistic models has been formulated considering that biotransformation could occur in both the liquid and the solid phase and that the biotransformation kinetic constants can be equal ($k_{bw} = k_{bs}$) or different ($k_{bw} \neq k_{bs}$) in both phases. Except for the model describing solid sequestration of the OMP, considering that the rates might be independent ($k_{bw} \neq k_{bs}$) does not provide a significant decrease of the fitting error, leading to slightly lower NRMSE values but higher AIC (Table 2). Therefore, the additional model complexity related to independent biotransformation constants does not seem to be justified and will henceforth only be retained for the sequestration model.

Comparing the different mechanistic models with the pseudo-first order model (Table 2), the Michaelis-Menten hypothesis did not improve the fitting of any compound, and the inhibition model decreased the NRMSE of FLX but increased the error of SMX, which is highly biotransformed and thus the model predicts an inhibition above reality (Figures S3). Therefore, these mechanisms seem to be not adequate to explain the biotransformation of OMPs. On the contrary, the models considering a reversible

biotransformation or a sequestration of the OMPs improve the fitting of the experimental data with respect to the pseudo-first order model (Table 2, Figure 3). More importantly, only the kinetic profiles of those two models are able to reproduce biotransformation trends that slow down steadily (Figure S3). This improvement with respect to the pseudo-first order model appears significant for compounds with a medium or high hydrophobicity, as FLX and E1+E2, while the fitting of ERY and SMX was very similar (Figure 3). This fact does not imply that the biotransformation of ERY and SMX cannot be explained by these mechanisms, but since they did not present a clear plateau either the chemical equilibrium constant is very high or sequestration is negligible. In this section, the differences found between the reversible biotransformation and the sequestration model (i.e., AIC, Table 2) are not enough to discriminate between both.

Table 2. Comparison of the normalized root mean square errors (NRMSE) and the Akaike Information Criterion (AIC) obtained during calibration (Experiments 1-2) of four representative compounds for the 10 formulated models.

		NRMSE (%)				AIC			
		FLX	E1+E2	ERY	SMX	FLX	E1+E2*	ERY	SMX
$k_{bw} = k_{bs}$	Pseudo-first order	8.06	4.87	3.49	4.24	123	4.5	76	87
	Michaelis-Menten	8.36	4.89	3.54	4.44	127	6.7	79	91
	Inhibition by TP	6.10	5.08	4.23	9.19	109	8.9	89	132
	Reversible biotransf.	4.29	2.52	3.39	4.21	89	-30	76	89
	Bioav.-Sequestration	5.11	3.92	3.52	4.26	101	-3.6	80	91
$k_{bw} \neq k_{bs}$	Pseudo-first order	8.01	4.87	3.48	4.24	125	6.2	78	89
	Michaelis-Menten	8.24	4.89	3.52	4.44	128	9.0	81	93
	Inhibition by TP	6.13	4.23	3.72	4.73	112	0.6	84	97
	Reversible biotransf.	4.29	2.52	3.39	4.21	91	-28	78	91
	Bioav.-Sequestration	4.30	2.35	3.47	4.23	94	-30	82	93

*The AIC values of E1+E2 are lower than the other OMPs because their initial concentration was 20 µg/L instead of 100 µg/L.

Pseudo-first order *Reversible biotransformation* *Bioavailability-sequestration*

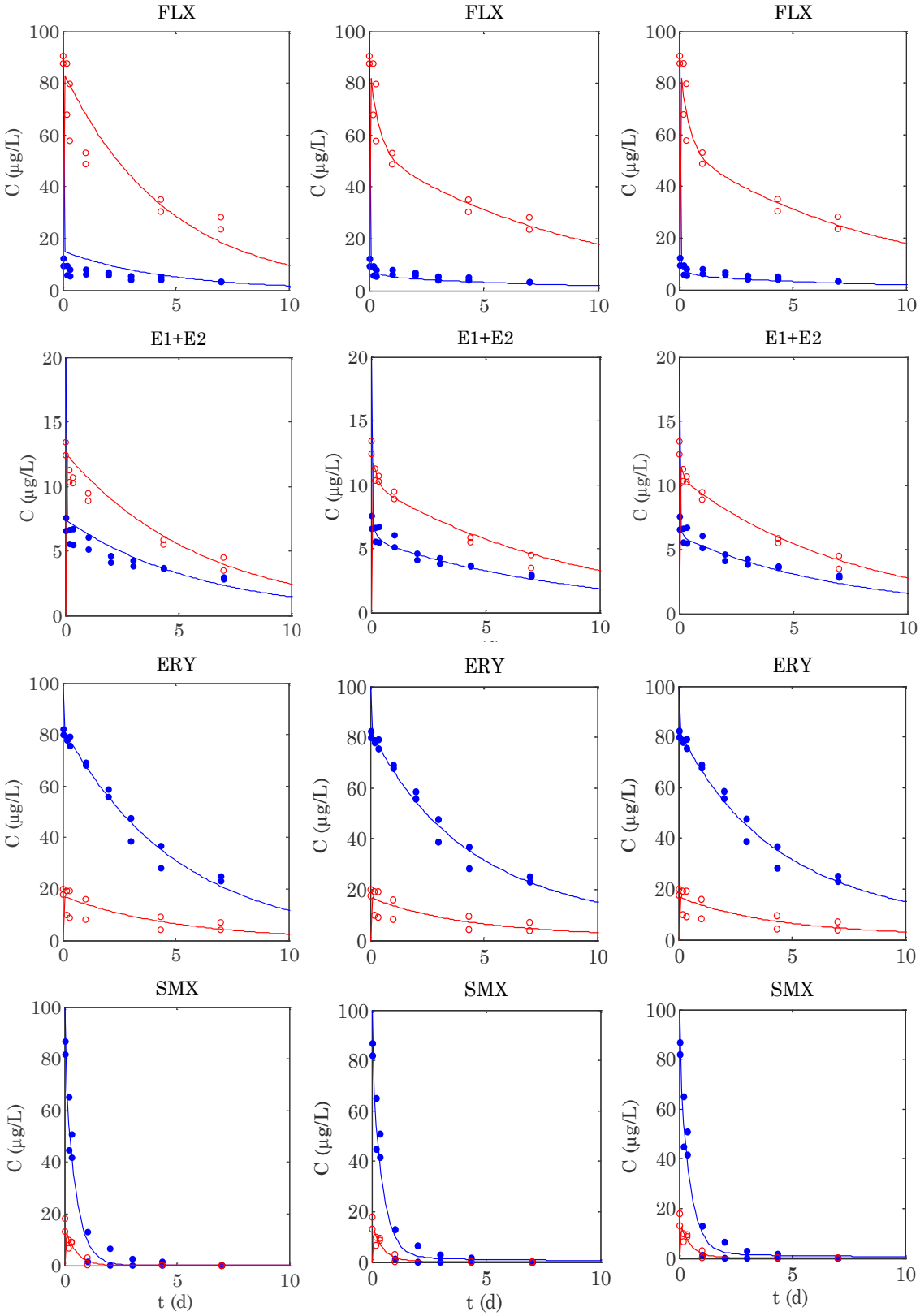

Figure 3. Experimental (dots) and modelled (lines) concentrations of methanogenic Experiments 1-2. Red and blue colors refer to the concentration in the solid and liquid phase, respectively.

4.2 Model calibration for methanogenesis

In order to find which of the two selected models in the previous section is more appropriate for the 20 OMPs, both models were robustly calibrated following a bootstrap procedure. The estimated parameters of the reversible biotransformation and sequestration models are shown in Table 3 and Table 4, respectively, with their corresponding confidence interval of 95%. Figure 3 and Figure S4 compare for all the OMP the fitting of these two models versus the pseudo-first order model. It should be pointed out that Experiments 1-2 were conducted in a continuous reactor, and thus washout of OMPs partially hides the concentration plateaus of Figure 3 and Figure S4.

To evaluate the biotransformation in the reversible model, the ratio between the direct and reverse biotransformation constants should be considered. As expected, compounds with higher biotransformation efficiency (Table 1), i.e. SMX and TMP, presented the highest ratio ($k_b/k_{rev} > 3$) while the persistent compounds, as DCF ($k_b/k_{rev} = 0.06$), had a lower ratio. The values of the biotransformation and reversible constants highlight that this mechanism is more relevant for compounds of Groups 1 and 2, which have a medium k_b but a superior k_{rev}. Consequently, these OMPs improve the fitting with respect to the pseudo-first order model in a higher extent than those of Group 3 and 4 (Figure S4 and Table S7), which did not show such a marked concentration plateau.

Similarly, simulated data with the sequestration model fitted particularly well the experimental values of compounds of Group 1 and 2 (Figure S4 and Table S7). As expected, the estimation of the partition coefficient is almost the same in both models. It should be noticed that the absolute values of k_{seq} and k_{desq} are not sufficient to determine the influence of sequestration on the OMP fate, and neither the k_{seq}/k_{desq} ratio. Actually, the hydrophobicity and the sequestrability of the OMPs cannot be analyzed independently. For instance, the effect of sequestration on the model will be different for

two OMPs with the same k_{seq}/k_{desq} ratio but different K_d values. Therefore, the mathematical impact of a single model parameter should not be considered by itself, but in the context of the overall model.

Graphical inspection (Figure S3 and Figure S4), the average NRMSE for an OMP ($\overline{NRMSE}$) and the total AIC confirm that specially the reversible biotransformation model ($\overline{NRMSE}$ = 4.40%, AIC = 1722), but also the sequestration model ($\overline{NRMSE}$ = 4.40%, AIC = 1810) fit better the experimental data than the pseudo-first order model ($\overline{NRMSE}$ = 6.64%, AIC = 1962). However, the slight differences in these three criteria do not allow making a definitive model selection between both models.

Table 3. Estimated parameters of the reversible biotransformation model calibrated with the methanogenic Experiments 1-2 and resulting normalized root mean square errors (NRMSE) for each compound and on average ($\overline{NRMSE}$). The estimated values are reported with the corresponding lower (LB) and upper boundaries (UB) of their confidence interval ($\alpha = 0.05$).

	OMPs	k_{sor} (L/gTSS d)		K_d (L/gTSS)		k_b (L/gVSS d)		k_{rev} (L/gVSS d)		NRMSE (%)
		Mean	[LB, UB]	Mean	[LB, UB]	Mean	[LB, UB]	Mean	[LB, UB]	
Group 1	**FLX**	**92**	**[26, 294]**	**1.03**	**[0.839, 1.27]**	**0.328**	**[0.182, 0.508]**	**0.492**	**[0.219, 0.944]**	**4.29**
	TCS	112	[38, 308]	20.4	[5.9, 31.6]	0.204	[0.168, 0.244]	0.291	[0.225, 0.377]	2.04
	NP	117	[28, 316]	28.9	[3.9, 31.6]	0.077	[0.045, 0.122]	0.115	[0.027, 0.212]	3.59
	OP	87	[33, 296]	31.3	[29.6, 31.6]	0.232	[0.173, 0.286]	0.154	[0.096, 0.244]	3.81
	TON	75	[32, 226]	31.0	[21.8, 31.6]	0.125	[0.086, 0.168]	0.194	[0.105, 0.299]	3.51
	GLX	106	[38, 310]	24.3	[6.9, 31.6]	0.191	[0.157, 0.228]	0.226	[0.154, 0.294]	2.62
	CEL	35	[30, 46]	18.3	[5.7, 31.6]	0.172	[0.140, 0.205]	0.220	[0.158, 0.298]	2.51
Group 2	**E1+E2**	**103**	**[29, 303]**	**0.189**	**[0.179, 0.199]**	**0.277**	**[0.133, 0.523]**	**0.987**	**[0.384, 2.20]**	**2.52**
	EE2	106	[25, 310]	0.236	[0.224, 0.251]	0.288	[0.117, 0.660]	0.983	[0.308, 2.79]	2.26
	DZP	51	[12, 292]	0.095	[0.088, 0.103]	0.136	[0.065, 0.297]	0.413	[0.144, 1.20]	3.07
	BPA	158	[40, 314]	0.150	[0.133, 0.167]	0.182	[0.068, 0.324]	0.495	[0.098, 0.995]	5.36
	CBZ	8.8	[5.7, 18]	0.064	[0.057, 0.071]	0.937	[0.433, 1.47]	2.17	[0.904, 3.16]	4.27
Group 3	**ERY**	**65**	**[8, 279]**	**0.022**	**[0.019, 0.025]**	**0.036**	**[0.026, 0.048]**	**0.031**	**[0.001, 0.078]**	**3.39**
	ROX	51	[12, 232]	0.061	[0.058, 0.064]	0.045	[0.028, 0.070]	0.131	[0.051, 0.301]	2.66
	DCF	77	[5, 300]	0.024	[0.020, 0.028]	0.089	[0.003, 0.267]	1.44	[0.263, 3.16]	4.95
	NPX	80	[2, 303]	0.037	[0.021, 0.060]	1.66	[0.365, 3.95]	1.32	[0.079, 3.16]	15.1
	IBP	90	[3, 315]	0.024	[0.020, 0.028]	0.018	[0.005, 0.053]	0.069	[0.000, 0.315]	4.98
G. 4	**SMX**	**16**	**[2, 175]**	**0.020**	**[0.016, 0.024]**	**0.690**	**[0.561, 0.797]**	**0.014**	**[0.000, 0.053]**	**4.21**
	TMP	62	[4 313]	0.038	[0.029, 0.048]	0.275	[0.146, 0.473]	0.075	[0.000, 0.236]	8.52
	$\overline{NRMSE}$									**4.40**

Table 4. Estimated parameters of the bioavailability-sequestration model calibrated with methanogenic Experiments 1-2 and resulting normalized root mean square errors (NRMSE) for each compound and on average ($\overline{NRMSE}$). The estimated values are reported with the corresponding lower (LB) and upper boundaries (UB) of their confidence interval ($\alpha = 0.05$).

	OMPs	k_{sor} (L/gTSS d)		K_d (L/gTSS)		k_{bw} (L/gVSS d)		k_{bs} (L/gVSS d)		k_{seq} (L/gVSS d)		k_{desq} (1/d)		NRMSE (%)
		Mean	[LB, UB]	Mean	[LB, UB]	Mean	[LB, UB]	Mean	[LB, UB]	Mean	[LB, UB]	Mean	[LB, UB]	
Group 1	**FLX**	**65**	**[27, 218]**	**1.03**	**[0.879, 1.25]**	**0.023**	**[0.000, 0.160]**	**0.377**	**[0.230, 0.630]**	**0.182**	**[0.069, 0.449]**	**0.034**	**[0.000, 0.196]**	**4.30**
	TCS	70	[38, 120]	23.9	[8.3, 31.6]	0.037	[0.000, 0.596]	0.204	[0.172, 0.237]	0.087	[0.065, 0.132]	0.015	[0.000, 0.108]	2.01
	NP	81	[28, 191]	29.8	[8.2, 31.6]	0.003	[0.000, 0.017]	0.084	[0.055, 0.133]	0.040	[0.017, 0.084]	0.053	[0.000, 0.423]	3.63
	OP	62	[33, 108]	31.0	[29.4, 31.6]	0.001	[0.000, 0.004]	0.239	[0.195, 0.287]	0.048	[0.033, 0.079]	0.010	[0.000, 0.085]	3.80
	TON	54	[32, 100]	30.5	[13.4, 31.6]	0.070	[0.000, 1.22]	0.128	[0.089, 0.159]	0.059	[0.034, 0.099]	0.014	[0.000, 0.139]	3.46
	GLX	76	[38, 166]	27.2	[10.0, 31.6]	0.074	[0.000, 0.987]	0.189	[0.156, 0.236]	0.067	[0.047, 0.097]	0.005	[0.000, 0.056]	2.56
	CEL	35	[30, 44]	16.3	[5.8, 31.6]	0.004	[0.000, 0.012]	0.171	[0.139, 0.205]	0.062	[0.046, 0.088]	0.004	[0.000, 0.048]	2.43
Group 2	**E1+E2**	**180**	**[30, 315]**	**0.190**	**[0.180, 0.200]**	**0.036**	**[0.015, 0.057]**	**0.702**	**[0.358, 1.27]**	**0.736**	**[0.258, 1.48]**	**0.011**	**[0.000, 0.047]**	**2.36**
	EE2	45	[25, 115]	0.237	[0.226, 0.250]	0.052	[0.026, 0.075]	1.09	[0.370, 2.60]	1.31	[0.300, 3.46]	0.022	[0.002, 0.066]	1.92
	DZP	29	[12, 87]	0.095	[0.089, 0.102]	0.023	[0.000, 0.046]	0.449	[0.156, 1.04]	0.386	[0.046, 1.34]	0.015	[0.000, 0.111]	3.07
	BPA	117	[32, 308]	0.150	[0.131, 0.167]	0.020	[0.000, 0.067]	0.318	[0.136, 0.577]	0.199	[0.062, 0.414]	0.015	[0.000, 0.083]	5.35
	CBZ	9.2	[5.7, 15]	0.065	[0.058, 0.073]	0.003	[0.000, 0.026]	2.55	[1.13, 4.85]	0.711	[0.253, 1.50]	0.003	[0.000, 0.024]	4.21
Group 3	**ERY**	**46**	**[5, 273]**	**0.022**	**[0.019, 0.025]**	**0.034**	**[0.004, 0.044]**	**0.562**	**[0.006, 3.10]**	**1.21**	**[0.013, 5.06]**	**0.067**	**[0.000, 0.146]**	**3.47**
	ROX	43	[9, 284]	0.060	[0.056, 0.064]	0.029	[0.000, 0.041]	0.521	[0.138, 1.35]	0.957	[0.032, 2.51]	0.040	[0.000, 0.232]	2.78
	DCF	51	[3, 293]	0.024	[0.020, 0.029]	0.001	[0.000, 0.010]	0.648	[0.047, 2.88]	0.635	[0.059, 3.03]	0.003	[0.000, 0.026]	4.91
	NPX	63	[2, 300]	0.039	[0.024, 0.058]	0.070	[0.000, 0.255]	6.74	[1.69, 9.99]	0.699	[0.067, 1.82]	0.128	[0.000, 0.348]	15.2
	IBP	39	[4, 235]	0.023	[0.020, 0.027]	0.017	[0.004, 0.028]	0.278	[0.003, 1.48]	2.81	[0.142, 25.0]	0.184	[0.000, 0.374]	4.92
G. 4	**SMX**	**17**	**[2, 140]**	**0.020**	**[0.016, 0.025]**	**0.653**	**[0.080, 0.965]**	**0.953**	**[0.000, 4.53]**	**0.034**	**[0.000, 0.100]**	**0.030**	**[0.000, 0.100]**	**4.23**
	TMP	51	[3, 301]	0.038	[0.029, 0.049]	0.128	[0.000, 0.324]	1.23	[0.081, 4.05]	0.296	[0.003, 2.55]	0.190	[0.000, 1.208]	8.93
	$\overline{NRMSE}$													**4.40**

4.3 Model validation for methanogenesis

The reversible and the sequestration models were validated with an independent set of methanogenic data (Experiment 3, Figure 1). We compare their ability to simulate this independent experiment using the estimated parameters (Table 3 and Table 4) by comparing their validation NRMSE (Table S7), complexity (AIC) and graphical trends (Figure 4 and Figure S5) versus the pseudo-first order model.

The reversible and the sequestration models were capable of predicting satisfactorily the behavior of most OMPs under methanogenic conditions, thereby validating the previously obtained parameters, while the pseudo-first order model appears again as a poorer alternative. To evaluate the goodness of the predictions, it should be taken into account that the microbial populations and the biotransformation capacity of the methanogenic biomass could have changed in this independent experiment. As previously reported (Gonzalez-Gil et al., 2018), these differences were mainly significant for SMX, EE2, and NP; consequently, their predicted and experimental concentrations are quite far.

Despite the comparable $\overline{NRMSE}$ for the sequestration (8.15%) and reversible models (8.35%), the simulated biotransformation trend could be different, as can be observed for FLX, E1+E2, TCS, and NPX in Figure 4 and Figure S5. In these cases, visual inspection reveals that the reversible biotransformation model predicts their kinetic behavior in a more realistic way, although the NRMSE of both models are very similar (relative differences below 15%). Instead of the NRMSE, the AIC is a more reliable and realistic criteria for comparison of non-nested models with a different number of independent parameters. The AIC values support the reversible biotransformation hypothesis (1278 vs. 1324). Yet, according to the results obtained during calibration, the short differences (< 5%) in AIC values make complex to select the best model univocally.

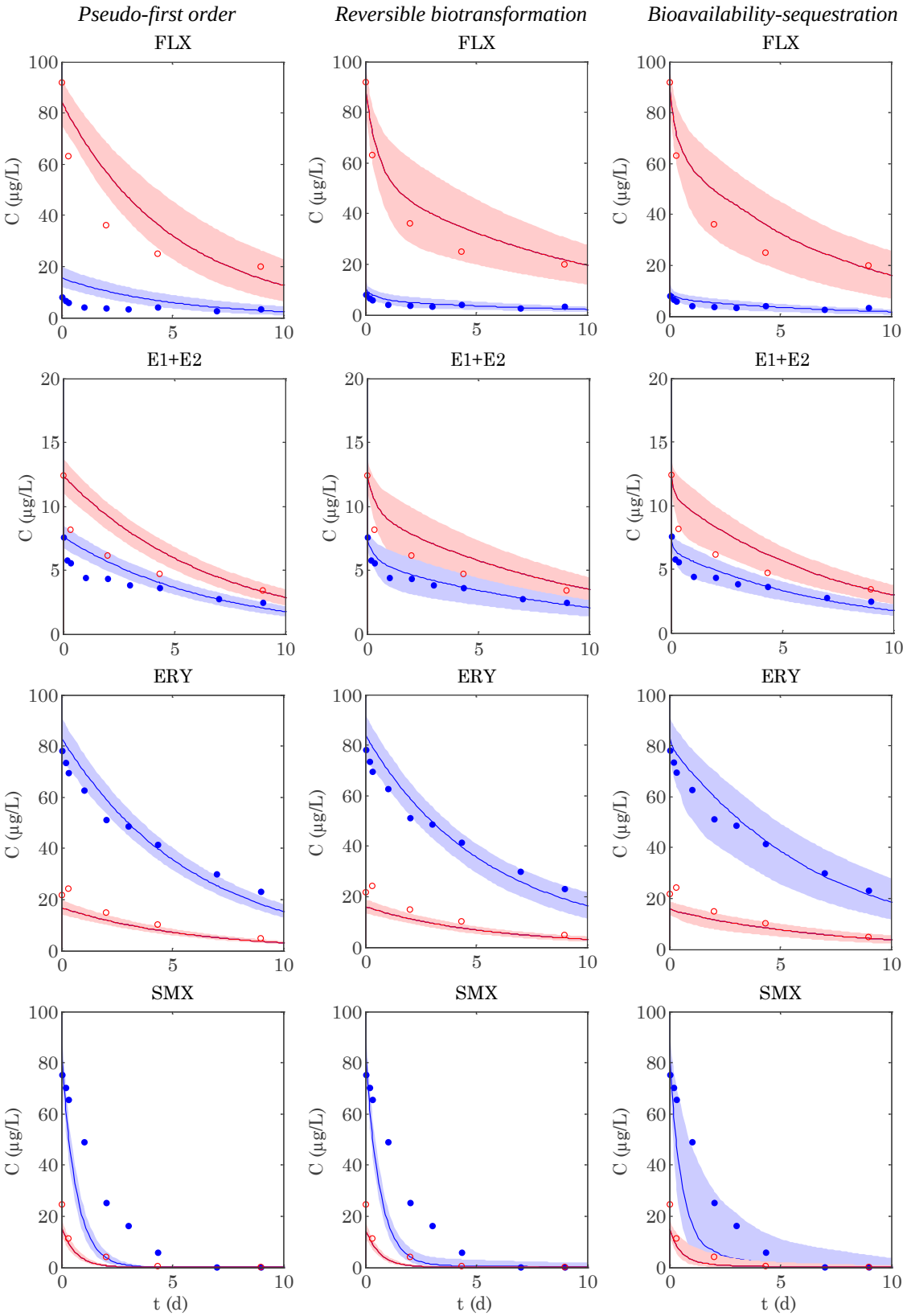

Figure 4. Validation of experimental concentrations (dots) using the mean parameters estimated during calibration (continuous lines) with methanogenic reactors. The colored areas represent the fate of the compound with a confidence interval of 95 % and were estimated with the parameters of the lower and upper boundaries (Table 3 and Table 4). Red and blue colors refer to the solid and liquid phase concentrations, respectively.

4.4 Mechanistic model verification in the overall anaerobic process

To confirm if the proposed mechanistic hypotheses are valid to explain the biotransformation in the overall anaerobic process, the pseudo-first order (as a reference), the reversible and sequestration models were calibrated with kinetic results from batch experiments performed with biomass from an anaerobic digester (Experiment 4, Figure 1). In this experiment, the biomass characteristics are different from those of the methanogenic experiments (Experiments 1-3) and hence a new set of parameters was estimated (data not shown).

Figure 5 and Figure S6 reveal that, again, the reversible and sequestration models are able to fit properly the experimental data, while the pseudo-first order model is unable to adjust the plateaus of OMP concentration. Even though for most OMPs there is no significant differences between both models, in the case of TON and NPX the sequestration model is more appropriate, while the reversible biotransformation reproduces better the behavior of BPA (Table S7 and Figure S6). Like in the methanogenic parameter validation, the reversible model leads to lower values of the total AIC (624 vs. 682) because it has fewer parameters, while the $\overline{NRMSE}$ are almost equal for both models (5.19% vs. 4.93%). Therefore, although the sequestration strength and/or some biotransformation reactions can be different in the overall anaerobic process from only in the methanogenic step, these two mechanisms are able to explain the incomplete biotransformation of OMPs.

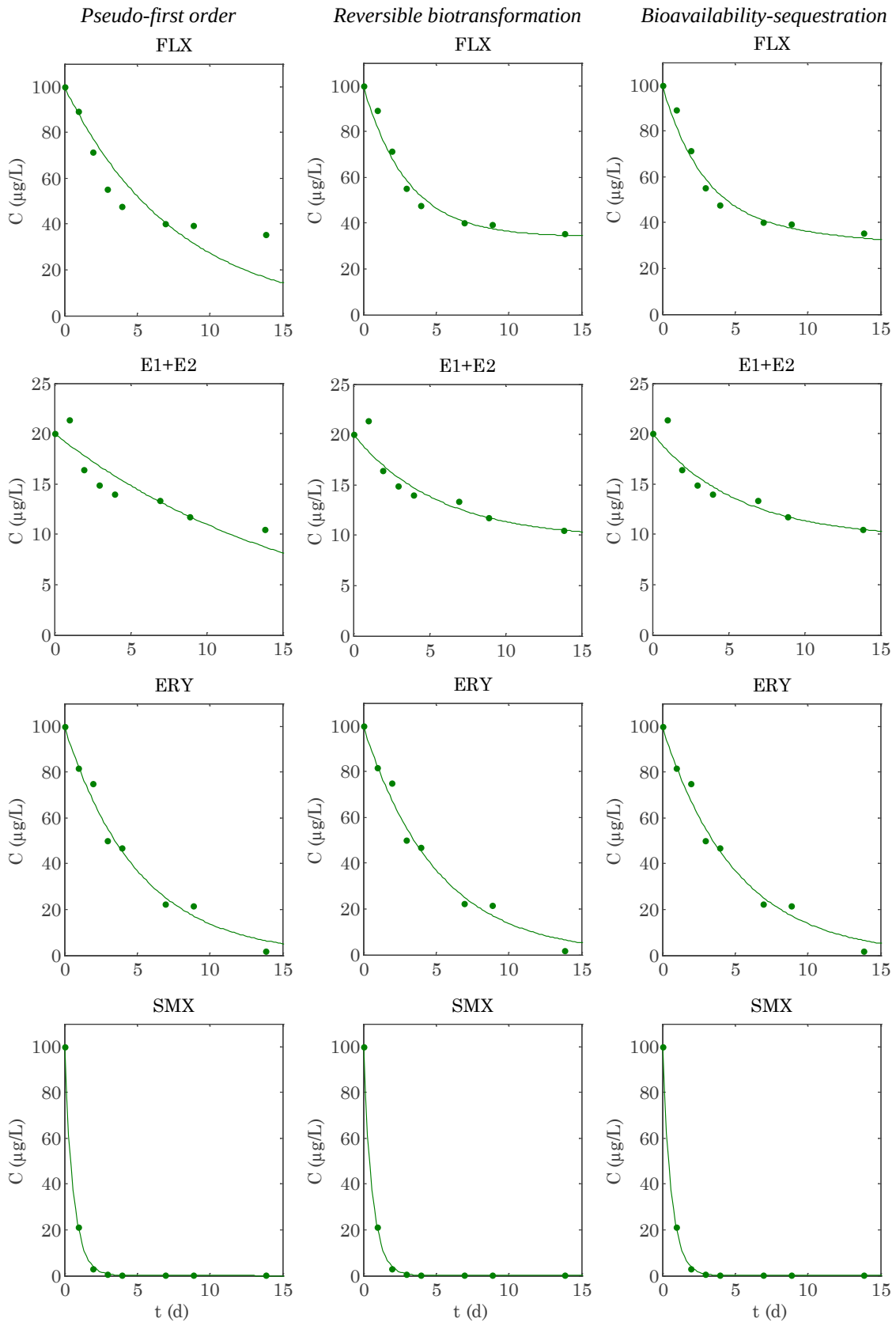

Figure 5. Experimental (dots) and modelled (lines) total concentrations obtained for four representative OMPs in anaerobic batch assays (Experiment 4).

5. DISCUSSION

5.1 Selection of the best model: reversible biotransformation vs. sequestration

Incomplete biotransformation of OMPs has been reported for several biological systems (Blair et al., 2015; Fernandez-Fontaina et al., 2014; Gonzalez-Gil et al., 2018; Gulde et al., 2018; Xue et al., 2010), but the reasons behind this behavior remain unknown. The use of mathematical models could be a useful tool for discerning the most likely hypothesis of biotransformation mechanisms; nevertheless, this methodology was rarely applied to anaerobic systems and it is only focused on PAH (Barret et al., 2010a, 2010b; Delgadillo-Mirquez et al., 2011). These available models consider that PAH biotransformation follows a cometabolic kinetic and that compounds are distributed in three sludge compartments (freely dissolved in the liquid phase, sorbed onto particles and sorbed onto dissolved/colloidal matter), which influence their bioavailability. However, the PAH physicochemical characteristics and behavior differ widely from the OMPs here investigated and no link between the substrate uptake rate and the OMP biotransformation was found at typical OLR for AD (Gonzalez-Gil et al., 2018). Therefore, new mechanistic models were proposed to understand the biotransformation limitations of OMPs.The results obtained in the present study reveal that reversibility of the biological reactions and/or a limited bioavailability of the compounds are likely mechanisms to explain the incomplete biotransformation in anaerobic systems. Although conceptually different, both models are based on thermodynamic restrictions assuming the existence of a “reservoir” of TP that can be turned into the parent OMP either by a reversible reaction, or by the desequestration. Despite the reversible model having fewer parameters and generally lower AIC values, the differences obtained with modelling criteria (NRMSE, AIC, graphical inspection) for the available experimental data are insufficient to clearly

discern which of the two mechanisms explains better the incomplete anaerobic biotransformation of OMPs.

There are already some studies focused on investigating the effect of the OMP bioavailability on its biotransformation that support the proposed sequestration mechanism. Aemig et al. (2016) noticed that the distribution of PAH in the organic matter of sewage sludge could be divided in readily, low, and non-accessible pools. The fate of the fraction present in accessible organic matter combines transfer from one pool to another together with anaerobic degradation, while the compounds in a low accessible compartment are poorly removed and they tend to accumulate in the non-accessible fraction. To enhance their removal, hydrolysis processes that increase the accessible fraction should be promoted. The authors propose that the distribution depends on the compound properties, the quantity/quality of organic matter in each pool and the aging phenomenon. These factors could justify some of the differences found between the methanogenic and overall anaerobic biotransformation. Moreover, in a recently published study, Gulde et al. (2018) go a step forward on investigating the OMPs bioavailability, proving that aliphatic amines undergo an irreversible ion trapping by the protozoa present in activated sludge and suggesting that this process could explain the experimental deviations that they observed from the first order kinetics. This mechanism is considered consistent with sequestration, and could be responsible for the incomplete biotransformation of some OMPs (e.g. FLX) in anaerobic systems, since ion trapping seems to increase for compounds with high pK_a and lipophilicity (Marceau et al., 2012) and because there are also protozoa present in anaerobic reactors (Priya et al., 2007). However, this mechanism is not able to explain why other compounds such as TON or IBP (not aliphatic amines), do not fit the pseudo-first order kinetic either.

There are also strong evidences to support the reversible biotransformation hypothesis. Any enzymatic reaction is reversible; nevertheless, if one reaction direction releases free energy ($\Delta G^{\circ} << 0$), it is much more favored than free energy-consuming reactions and they can be considered as irreversible ($k_b >> k_{rev}$, e.g. SMX, Table 3). On the contrary, reactions that do not present a clearly favored direction are recognized as reversible. For instance, dehydrogenases are enzymes that catalyze reversible reactions (Bisswanger, 2014) and several OMPs are known to undergo dehydrogenation reactions, such as the transformation of bezafibrate into a alkene (Helbling et al., 2010) and the formation of ketones or quinones from compounds with hydroxyl-groups, such as (di)hydroxyl-CBZ (Kaiser et al., 2014) and NP isomers (Fischer and Majewsky, 2014). Also other biological reactions affecting OMPs have been recognized as reversible; for example, the N-oxidation of tertiary amines such as venlafaxine (Gulde et al., 2016), the phosphorylation of BPA (Zühlke et al., 2016), and likely the phosphorylation of other OMPs with carboxyl and hydroxyl groups by the methanogenic enzyme acetate kinase (Gonzalez-Gil et al., 2017).

To elucidate the mechanism limiting the biotransformation of each OMP, further experiments aiming to identify the transformation products and to prove sequestration of compounds are needed. Indeed, with the available data both sequestration and/or reversible biotransformation are equally plausible and not even mutually exclusive mechanisms as they might be compound specific. However, from a pragmatic perspective, the reversible model could have a broader applicability spectrum, while the sequestration model could be more likely for lipophilic compounds. In accordance, we have selected the reversible biotransformation model as a useful tool to accurately predict the biotransformation of OMPs under anaerobic conditions.

5.2 Implications for process performance

Finding an appropriate model that describes the real fate of OMPs is not only useful to understand the mechanisms behind their biotransformation, but also to predict accurately their behavior when operational parameters are modified, i.e. as a tool to optimize the process performance, and to predict OMPs discharge into the environment. The evaluation of uncertainty is particularly relevant for decision-making (Gimeno et al., 2017) as it provides a realistic estimation of the efficiency of new operational scenarios and the compliance with environmental standards predicting, e.g. the expected and maximum concentration of OMP in liquid and solid sludge phases (Figure S7).

An interesting application is the assessment of the influence of the HRT on OMPs biotransformation efficiency: this case study was evaluated in this section with the parameters estimated by the reversible model (Experiments 1-2). Taking into account the uncertainty, Figure 6 suggests that increasing the HRT above 10 d does not imply an improvement on the biotransformation of most OMPs, except for ERY, which follows a pseudo-first order behavior. Therefore, it does not seem worthy to increase the typical HRT (20-30 d) of anaerobic digesters to improve OMP removal. This conclusion is in agreement with previous findings (Carballa et al., 2007; Gonzalez-Gil et al., 2016; Malmborg and Magnér, 2015; Yang et al., 2016). These observations are consistent with the mechanisms found as plausible in this work, namely that thermodynamic limitations, rather than kinetics, are the main responsible for the partial biotransformation of OMPs.

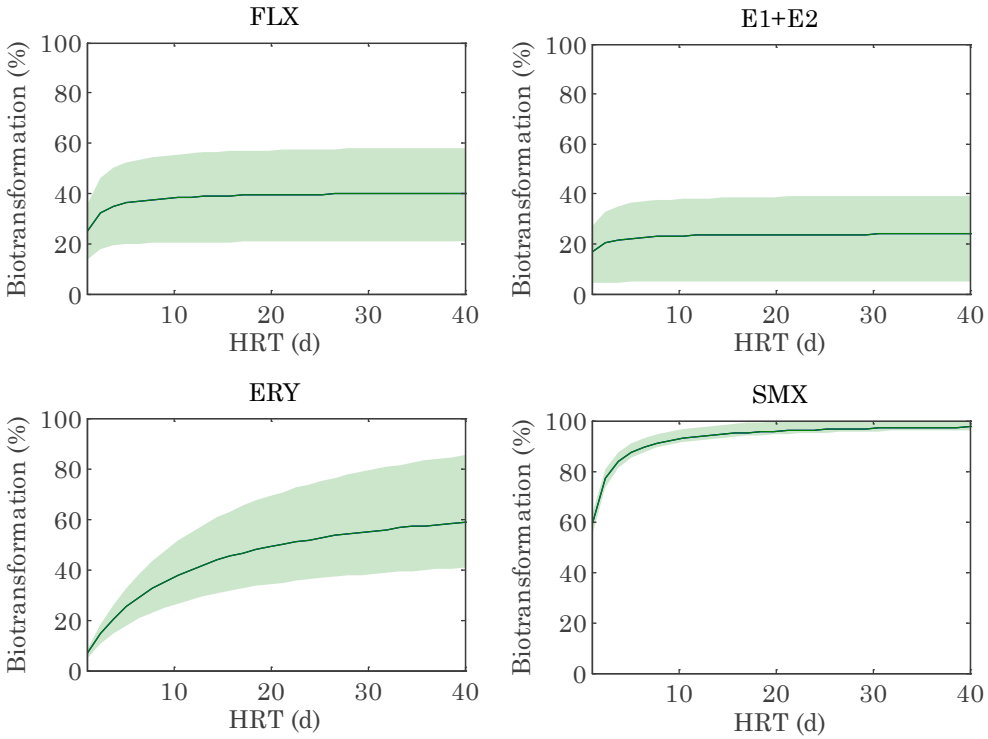

Figure 6. Predicted biotransformation efficiency of 4 representative OMPs in a methanogenic continuously stirred tank reactor at different HRT by the reversible model. The green area represents the uncertainty with a confidence range of 95%.

6. CONCLUSIONS

The mechanistic approach presented in this study allows not only to select a model that accurately predicts the fate of OMPs, but also to gain a further insight on the biotransformation mechanisms of OMPs in anaerobic systems, and likely in other biological systems. The combination of modelling and mechanistic criteria provided certain evidence that the reversibility of the biological reactions could lead to a chemical equilibrium between the parent compound and the TP, hence explaining why OMPs are not fully biotransformed. However, limited bioavailability of the compounds due to sequestration is also a plausible hypothesis of hindering the biotransformation of some OMPs. In sum, OMPs biotransformation is likely limited by thermodynamic rather than kinetic constraints. This information is crucial to avoid an overestimation of the

biotransformation capacity of the biomass (by using pseudo-first order models) and to asses operational strategies that really maximize the removal of OMPs. Future research should be focused on ultimately validate the reversible biotransformation and sequestration hypotheses by purposely designed experiments.

Acknowledgements

This research was funded by the Spanish Government (AEI) through the COMETT project (CTQ2016-80847-R) and by an FPU Grant (FPU13/01255). The authors belong to CRETUS Strategic Partnership (AGRUP2015/02) and to Galician Competitive Research Group (GRC ED431C 2017/29). All these programs are co-funded by FEDER (EU).

7. REFERENCES

Aemig, Q., Chéron, C., Delgenès, N., Jimenez, J., Houot, S., Steyer, J.P., Patureau, D., 2016. Distribution of Polycyclic Aromatic Hydrocarbons (PAHs) in sludge organic matter pools as a driving force of their fate during anaerobic digestion. Waste Manag. 48, 389–396.

Alvarino, T., Suarez, S., Lema, J.M., Omil, F., 2014. Understanding the removal mechanisms of PPCPs and the influence of main technological parameters in anaerobic UASB and aerobic CAS reactors. J. Hazard. Mater. 278, 506–513.

APHA, 2005. Standard Methods for the Examination of Water and Wastewater, 21st ed. American Public Health Association/American Water Works Association/Water Environment Federation, Washington DC, USA.

Banihashemi, B., Droste, R.L., 2014. Science of the Total Environment Sorption – desorption and biosorption of bisphenol A , triclosan , and 17 α -ethinylestradiol to sewage sludge. Sci. Total Environ. 487, 813–821.

Barret, M., Carrère, H., Delgadillo, L., Patureau, D., 2010a. PAH fate during the anaerobic digestion of contaminated sludge: Do bioavailability and/or cometabolism limit their biodegradation? Water Res. 44, 3797–3806.

Barret, M., Patureau, D., Latrille, E., Carrère, H., 2010b. A three-compartment model for micropollutants sorption in sludge: methodological approach and insights. Water Res. 44, 616–24.

Bisswanger, H., 2014. Enzyme assays. Perspect. Sci. 1, 41–55.

Blair, B., Nikolaus, A., Hedman, C., Klaper, R., Grundl, T., 2015. Evaluating the degradation, sorption, and negative mass balances of pharmaceuticals and personal

care products during wastewater treatment. Chemosphere 134, 395–401.

Brion, D., Pelletier, É., 2005. Modelling PAHs adsorption and sequestration in freshwater and marine sediments. Chemosphere 61, 867–876.

Byrns, G., 2001. The fate of xenobiotic organic compounds in wastewater treatment plants. Water Res. 35, 2523–2533.

Carballa, M., Omil, F., Ternes, T., Lema, J.M., 2007. Fate of pharmaceutical and personal care products (PPCPs) during anaerobic digestion of sewage sludge. Water Res. 41, 2139–50.

Chen, F., Ying, G.-G., Ma, Y.-B., Chen, Z.-F., Lai, H.-J., Peng, F.-J., 2014. Field dissipation and risk assessment of typical personal care products TCC, TCS, AHTN and HHCB in biosolid-amended soils. Sci. Total Environ. 470–471, 1078–86.

Criddle, C.S., 1993. The kinetics of cometabolism. Biotechnol. Bioeng. 41, 1048–1056.

Delgadillo-Mirquez, L., Lardon, L., Steyer, J.-P., Patureau, D., 2011. A new dynamic model for bioavailability and cometabolism of micropollutants during anaerobic digestion. Water Res. 45, 4511–21.

Falås, P., Wick, A., Castronovo, S., Habermacher, J., Ternes, T.A., Joss, A., 2016. Tracing the limits of organic micropollutant removal in biological wastewater treatment. Water Res. 95, 240–249.

Fernandez-Fontaina, E., Carballa, M., Omil, F., Lema, J.M., 2014. Modelling cometabolic biotransformation of organic micropollutants in nitrifying reactors. Water Res. 65, 371–383.

Fernandez-Fontaina, E., Gomes, I.B., Aga, D.S., Omil, F., Lema, J.M., Carballa, M., 2016. Biotransformation of pharmaceuticals under nitrification, nitratation and heterotrophic conditions. Sci. Total Environ. 541, 1439–1447.

Fischer, K., Majewsky, M., 2014. Cometabolic degradation of organic wastewater micropollutants by activated sludge and sludge-inherent microorganisms. Appl. Microbiol. Biotechnol. 98, 6583–6597.

Fountoulakis, M.S., Stamatelatou, K., Batstone, D.J., Lyberatos, G., 2006. Simulation of DEHP biodegradation and sorption during the anaerobic digestion of secondary sludge. Water Sci. Technol. 54, 119–128.

Frutiger, J., Marcarie, C., Abildskov, J., Sin, G., 2016. A Comprehensive Methodology for Development, Parameter Estimation, and Uncertainty Analysis of Group Contribution Based Property Models-An Application to the Heat of Combustion. J. Chem. Eng. Data 61, 602–613.

Gimeno, P., Marcé, R., Bosch, L., Comas, J., Corominas, L., 2017. Incorporating model uncertainty into the evaluation of interventions to reduce microcontaminant loads in rivers. Water Res. 124, 415–424.

Gonzalez-Gil, L., Carballa, M., Lema, J.M., 2017. Cometabolic Enzymatic Transformation of Organic Micropollutants under Methanogenic Conditions. Environ. Sci. Technol. 51, 2963–2971.

Gonzalez-Gil, L., Mauricio-Iglesias, M., Serrano, D., Lema, J.M., Carballa, M., 2018. Role of methanogenesis on the biotransformation of organic micropollutants during anaerobic digestion. Sci. Total Environ. 622–623, 459–466.

Gonzalez-Gil, L., Papa, M., Feretti, D., Ceretti, E., Mazzoleni, G., Steimberg, N., Pedrazzani, R., Bertanza, G., Lema, J.M., Carballa, M., 2016. Is anaerobic digestion effective for the removal of organic micropollutants and biological activities from sewage sludge? Water Res. 102, 211–220.

Grandclément, C., Seyssiecq, I., Piram, A., Wong-Wah-Chung, P., Vanot, G., Tiliacos, N., Roche, N., Doumenq, P., 2017. From the conventional biological wastewater treatment to hybrid processes, the evaluation of organic micropollutant removal: A review. Water Res. 111, 297–317.

Gulde, R., Anliker, S., Kohler, H.-P., Fenner, K., 2018. Ion trapping of amines in protozoa – a novel removal mechanism for micropollutants in activated sludge. Environ. Sci. Technol. acs.est.7b03556.

Gulde, R., Meier, U., Schymanski, E.L., Kohler, H.P.E., Helbling, D.E., Derrer, S., Rentsch, D., Fenner, K., 2016. Systematic Exploration of Biotransformation Reactions of Amine-Containing Micropollutants in Activated Sludge. Environ. Sci. Technol. 50, 2908–2920.

Helbling, D.E., Hollender, J., Kohler, H.-P.E., Singer, H., Fenner, K., 2010. High-throughput identification of microbial transformation products of organic micropollutants. Environ. Sci. Technol. 44, 6621–6627.

Helton, J.C., Davis, F.J., 2003. Latin hypercube sampling and the propagation of uncertainty in analyses of complex systems. Reliab. Eng. Syst. Saf. 81, 23–69.

Kaiser, E., Prasse, C., Wagner, M., Bröder, K., Ternes, T.A., 2014. Transformation of oxcarbazepine and human metabolites of carbamazepine and oxcarbazepine in wastewater treatment and sand filters. Environ. Sci. Technol. 48, 10208–10216.

Krah, D., Ghattas, A.-K., Wick, A., Bröder, K., Ternes, T. a., 2016. Micropollutant degradation via extracted native enzymes from activated sludge. Water Res. 95, 348–360.

Liu, L., Binning, P.J., Smets, B.F., 2015. Evaluating alternate biokinetic models for trace pollutant cometabolism. Environ. Sci. Technol. 49, 2230–2236.

Lolas, I.B., Chen, X., Bester, K., Nielsen, J.L., 2012. Identification of triclosan-degrading bacteria using stable isotope probing, fluorescence in situ hybridization and microautoradiography. Microbiology 158, 2796–2804.

Luo, Y., Guo, W., Ngo, H.H., Nghiem, L.D., Hai, F.I., Zhang, J., Liang, S., Wang, X.C., 2014. A review on the occurrence of micropollutants in the aquatic environment and their fate and removal during wastewater treatment. Sci. Total Environ. 473–474, 619–41.

Malmborg, J., Magnér, J., 2015. Pharmaceutical residues in sewage sludge: Effect of sanitization and anaerobic digestion. J. Environ. Manage. 153, 1–10.

Marceau, F., Bawolak, M.-T., Lodge, R., Bouthillier, J., Gagné-Henley, A., René, C., Morissette, G., 2012. Cation trapping by cellular acidic compartments: beyond the concept of lysosomotropic drugs. Toxicol. Appl. Pharmacol. 259, 1–12.

Meyers, R.A., 1995. Molecular biology and biotechnology: a comprehensive desk reference. John Wiley & Sons.

Nikaido, H., Vaara, M., 1985. Molecular basis of bacterial outer membrane permeability. Microbiol. Rev. 49, 1–32.

Paterakis, N., Chiu, T.Y., Koh, Y.K.K., Lester, J.N., McAdam, E.J., Scrimshaw, M.D., Soares, A., Cartmell, E., 2012. The effectiveness of anaerobic digestion in removing estrogens and nonylphenol ethoxylates. J. Hazard. Mater. 199–200, 88–95.

Polesel, F., Torresi, E., Loreggian, L., Casas, M.E., Christensson, M., Bester, K., Plósz, B.G., 2017. Removal of pharmaceuticals in pre-denitrifying MBBR – Influence of organic substrate availability in single- and three-stage configurations. Water Res. 123, 408–419.

Pomiès, M., Choubert, J.-M., Wisniewski, C., Coquery, M., 2013. Modelling of micropollutant removal in biological wastewater treatments: a review. Sci. Total Environ. 443, 733–48.

Priya, M., Haridas, A., Manilal, V.B., 2007. Involvement of protozoa in anaerobic wastewater treatment process. Water Res. 41, 4639–4645.

Stasinakis, A.S., 2012. Review on the fate of emerging contaminants during sludge anaerobic digestion. Bioresour. Technol. 121, 432–40.

Suárez, S., Carballa, M., Omil, F., Lema, J.M., 2008. How are pharmaceutical and personal care products (PPCPs) removed from urban wastewaters? Rev. Environ. Sci. Biotechnol. 7, 125–138.

Tiwari, B., Sellamuthu, B., Ouarda, Y., Drogui, P., Tyagi, R.D., Buelna, G., 2017. Review on fate and mechanism of removal of pharmaceutical pollutants from wastewater using biological approach. Bioresour. Technol. 224, 1–12.

Tousova, Z., Oswald, P., Slobodnik, J., Blaha, L., Muz, M., Hu, M., Brack, W., Krauss, M., Di Paolo, C., Tarcai, Z., 2017. European demonstration program on the effect-based and chemical identification and monitoring of organic pollutants in European surface waters. Sci. Total Environ. 601, 1849–1868.

Urase, T., Kikuta, T., 2005. Separate estimation of adsorption and degradation of pharmaceutical substances and estrogens in the activated sludge process. Water Res. 39, 1289–300.

Völker, J., Vogt, T., Castronovo, S., Wick, A., Ternes, T.A., Joss, A., Oehlmann, J., Wagner, M., 2017. Extended anaerobic conditions in the biological wastewater treatment: Higher reduction of toxicity compared to target organic micropollutants. Water Res. 116, 220–230.

Xue, W., Wu, C., Xiao, K., Huang, X., Zhou, H., Tsuno, H., Tanaka, H., 2010. Elimination and fate of selected micro-organic pollutants in a full-scale anaerobic/anoxic/aerobic process combined with membrane bioreactor for municipal wastewater reclamation. Water Res. 44, 5999–6010.

Yang, S., Hai, F.I., Price, W.E., McDonald, J., Khan, S.J., Nghiem, L.D., 2016. Occurrence of trace organic contaminants in wastewater sludge and their removals by anaerobic digestion. Bioresour. Technol. 210, 153–159.

Zühlke, M.K., Schlüter, R., Henning, A.K., Lipka, M., Mikolasch, A., Schumann, P., Giersberg, M., Kunze, G., Schauer, F., 2016. A novel mechanism of conjugate formation of bisphenol A and its analogues by Bacillus amyloliquefaciens: Detoxification and reduction of estrogenicity of bisphenols. Int. Biodeterior. Biodegrad. 109, 165–173.